LANGMUIR
Cite This: *Langmuir* 2019, 35, 4182−4188
Article
pubs.acs.org/Langmuir

Viscous Fingering Induced by a pH-Sensitive Clock Reaction

D. M. Escala,[†] A. De Wit,[‡] J. Carballido-Landeira,[§] and A. P. Muñuzuri*[,†]

[†]Group of Nonlinear Physics, Universidade de Santiago de Compostela, E-15782 Santiago de Compostela, Spain

[‡]Nonlinear Physical Chemistry Unit, Service de Chimie Physique et Biologie Théorique, Université libre de Bruxelles (ULB), CP231, Campus Plaine, 1050 Brussels, Belgium

[§]Facultad de Ciencias, Departamento de Física, Universidad de Oviedo, Campus de Llamaquique, C/Calvo Sotelo, s/n, 33007 Oviedo, Spain

Supporting Information

ABSTRACT: A pH-changing clock chemical system, also known to induce changes in viscosity, is shown experimentally to induce a viscous fingering instability during the displacement of reactive solutions in a Hele-Shaw cell. Specifically, a low-viscosity solution of formaldehyde is displaced by a more viscous solution of sulfite and of a pH-sensitive poly(acrylic acid) polymer. The pH change triggered by the formaldehyde−sulfite clock reaction in the reactive contact zone between the two solutions affects the polymer and induces a local increase of the viscosity that destabilizes the displacement via a viscous fingering instability. The influence of changes in the chemical parameters on this fingering instability is analyzed using different techniques and the results are compared with numerical simulations.

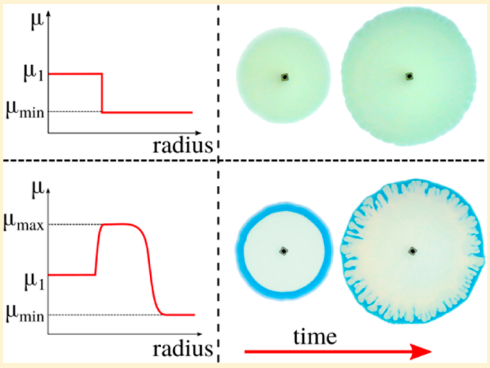

INTRODUCTION

Research in pH-sensitive materials is a major subject in science due to possible applications in a broad variety of fields. Just to name a few, many innovative medical therapies are focused on the use of pH-responsive systems to test drug-targeting techniques.[1,2] Recently, several experimental studies have reported the possibility to control and modulate the hydrodynamic viscous fingering instability by using chemical neutralization reactions coupled with pH-sensitive polymers[3−7] or polymerization reactions.[8,9] Viscous fingering typically occurs when a low-viscosity solution displaces a more viscous one and leads to increased mixing between the two liquids. It can be detrimental in chemical[10] and petroleum[3,11] applications, which explains the experimental[3−9] and theoretical[12,13] efforts devoted to control this hydrodynamic instability by in situ chemically driven viscosity changes.[3,4]

Recently, it has been shown that pH-sensitive materials can also be coupled with more complex pH-changing chemical reactions such as clock reactions and pH oscillators.[14−16] In particular, it has been shown that a clock-type change in the viscosity of a liquid can be obtained by coupling a pH-sensitive polymer (poly(acrylic acid), PAA) with a pH-changing clock reaction.[17] This paves the way to a more sensitive control of viscous fingering using the power of nonlinear chemical reactions[18,19] to modulate the viscosity in situ both in time and space.

In this context, we study here both experimentally and numerically chemically induced viscous fingering occurring when a low-viscosity solution of formaldehyde is displaced radially in a confined geometry at a fixed flow rate by a more viscous solution of sodium sulfite and PAA. The formaldehyde−sulfite (FS) system is a typical example of a nonlinear chemical reaction exhibiting a clock behavior in batch systems featuring large and well-controlled changes in pH.[14,17] pH-sensitive PAA has been shown, in a batch reactor, to be able to produce viscosity changes depending on the pH changes.[17] We explore here the possibility to use this reactive feedback on viscosity to trigger and control viscous fingering by changing the control parameters of the hydrodynamics and the chemistry involved.

Experiments are performed in a Hele-Shaw cell (two glass plates separated by a thin gap). Initially, no reaction can occur as the cell is filled only with formaldehyde solution. At the beginning of the experiment, a fixed volume of a more viscous solution of sulfite and PAA is injected into the system. This first displacement is hydrodynamically stable. Upon contact during a given time with no further injection between the two reactants of the FS clock reaction in the cell, a local change in pH is triggered, which generates in situ a non-monotonic viscosity profile with a maximum. When injection starts again, a viscous fingering instability can then be observed depending on the concentrations of the reactants.

This chemically driven fingering is analyzed experimentally for a broad range of flow rates and conditions. The reactivity of the system was modulated by varying the initial concentrations of the main reagents (sulfite and formaldehyde), whereas the

Received: November 14, 2018
Revised: January 31, 2019
Published: February 13, 2019

DOI: 10.1021/acs.langmuir.8b03834
Langmuir 2019, 35, 4182−4188

hydrodynamics was controlled by varying the flow rate. Advanced optical techniques are also used to detect the index of refraction gradients to unveil the mechanism behind the generation of the more viscous zone of reaction where the fingers are produced. In particular, it was observed that polymer aggregation is essential for the finger formation. Nonlinear simulations of the detailed kinetics of the FS reaction allow to construct reaction−diffusion pH profiles and hence the related viscosity profiles. When coupled to a flow model of fingering, numerical results of the convective instability present a good qualitative agreement with the experiments.

MATERIALS AND METHODS

Experimental Section. The low-viscosity displaced solution is an aqueous solution of formaldehyde prepared by directly diluting a commercial formalin solution by double-distilled water in appropriate proportions. The high-viscosity displacing solution was prepared by mixing stocks of poly(acrylic acid) (PAA), sodium sulfite, and a pH indicator as follows: 1 g of reagent-grade PAA (Sigma) with an average molecular weight of 4×10^6 g/mol was diluted into 180 mL of double-distilled water at 80 °C to facilitate solubility. Then, the mixture was cooled down to 23 °C and the final volume was brought to 200 mL to obtain a PAA stock solution of 0.5 wt %. The sodium sulfite stock solution was prepared by diluting 25.21 g of reagent-grade Na_2SO_3 (Sigma) in 100 mL of double-distilled water bubbled with argon to avoid oxidation. The pH color indicator (hereafter CI) used for these experiments is a 0.4% hydroalcoholic solution of Bromothymol blue prepared by dissolving 1 g of Bromothymol blue sodium salt powder (Sigma) into 50 mL of 96% ethanol solution diluting up to a final volume of 250 mL by adding 200 mL of double-distilled water. The CI shows a yellow color for pH values below 6 (acidic state), a green color for pH between 6 and 7 (neutral state), and a blue color for pH values above 7 (basic state).[20] The complete characterization of the clock reaction as well as the rheological properties of the polymer solution have been reported elsewhere.[17] To rule out any artifact in the results due to the elastic property of the polymer solution, the first normal stress difference (N_1) of the mixture and the shear rate inside the Hele-Shaw were measured. This information can be consulted in the Supporting Information (SI).

The sketch of the experimental setup is shown in Figure 1. The Hele-Shaw cell was built using two square glass plates (25 cm × 25 cm) separated by a poly(tetrafluoroethylene) frame of 0.25 mm thickness. The horizontal cell was initially filled with the displaced solution. The displacing PAA/sulfite solution was injected through a 4 mm hole located at the geometric center of the bottom plate using a syringe pump (kdScientific: Legato 200 series). All experiments were recorded from above using a charge-coupled device (CCD) camera (PixeLINK: PL-B776U) connected to a computer. The samples were illuminated from below using a rectangular light-emitting diode pad and a light diffuser (Figure 1a). The image postprocessing was done with the GNU software FIJI.[21] Some experiments were also performed using a Schlieren technique (Figure 1b) to track changes in the optical index of refraction of the solutions induced by fluid movements that cannot be observed by a direct optical inspection.[8,9,22] To perform the Schlieren measurements, the Hele-Shaw cell was placed between two collimator lenses. The system was illuminated using a pinhole-led light source. An iris cutoff filter was located at the focus point between the CCD and the collimator lens.[22,23] To start the experiment, the formaldehyde solution is first displaced by 3 mL of PAA/sulfite solution at an injection flow rate of 7 mL/min. Then, the injection is stopped and the chemicals are allowed to diffuse and the reaction to take place in the miscible reaction zone between both solutions during 3 h. After this time (indicated as t = 0 s in Figure 2), injection is started again and the viscous fingering instability is studied by injecting 3 mL of the displacing solution at four different flow rates Q (2.5, 7, 10, and 20 mL/min).

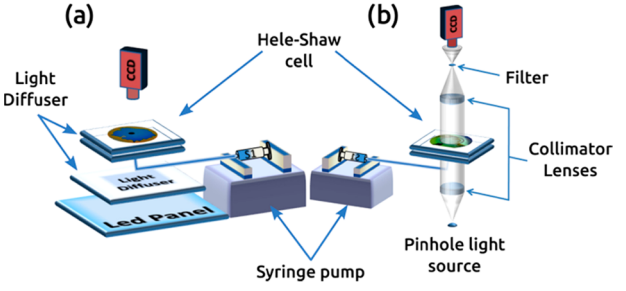

Figure 1. Schematics of the experimental setup. (a) Configuration for visible light detection (colored experiments). (b) Schlieren arrangement for optical detection of gradients of index of refraction in the absence of color indicator.

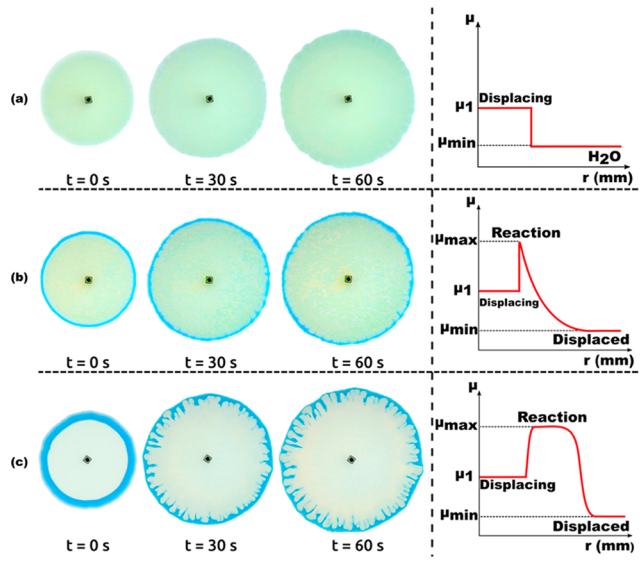

Figure 2. Comparison of three experiments where the $[\text{formaldehyde}]_0$ in the displaced solution is (a) 0 M, (b) 0.0496 M, and (c) 0.75 M. In all three cases, the concentrations of other reagents were kept constant at $[PAA]_0$ = 0.4386 wt %, $[SO_3^{2-}]_0$ = 0.0684 M, and $[CI]_0$ = 0.021 wt %. The displacing solution was injected at a flow rate of 7 mL/min after obtaining the initial condition as described in the Materials and Methods section. In the last column, schematic profiles corresponding to each initial condition are shown, indicating the minimum (μ_{min}), maximum (μ_{max}), and displacing solution (μ_1) viscosities.

Numerical Methods. Numerical simulations are produced integrating the reaction model described by Kovacs et al.[14] The initial condition for the simulations was obtained in a similar way as in the experiments. First, a one-dimensional (1D)-reaction−diffusion simulation was performed by locating the required reagents into the proper spatial coordinates following the experimental procedure. In the absence of convection, the final concentration profiles were obtained by solving the following reaction−diffusion equations

$$\partial_t C_i = D_i \nabla^2 C_i + R_i(C_i) \quad (1)$$

where C_i represents the concentration of species i included in the chemical model in Table S1. D_i is the diffusion coefficient for each species. Diffusion coefficients[24] were set as $D_D = 1 \times 10^{-9}$ m^2/s for all reagents in the displaced solution (lower viscosity) and $D_R = 1 \times 10^{-11}$ m^2/s for all reagents in the displacing solution (higher viscosity) and R_i represents the reaction term. The reaction equations and the rate constants are in Table S1. A mass action rate law was used to

DOI: 10.1021/acs.langmuir.8b03834
Langmuir 2019, 35, 4182−4188

calculate the rate equations in all cases. The 1D spatial profiles of H^+ and OH^- obtained in this way were then mapped into a two-dimensional (2D) space by simply rotating it around the origin, and it was taken as the initial condition for the diffusion−convection simulation.

With the initial condition obtained, the nonlinear diffusion−convection simulations were performed using a second-order finite-element method approximation.[25] The system dynamics were modeled by implementing Darcy's law for the flow velocity simulated in Ansys Fluent 18.1. A 2D circular domain was discretized using a structured mesh of regular elements (see the Supporting Information for additional details on the selection of the grid mesh size and validation of the model). The equations solved are

$$\bar{\nabla}\cdot\bar{u} = 0 \tag{2}$$

$$\bar{\nabla}\cdot p = -\frac{\mu(r)\cdot\bar{u}}{\kappa} \tag{3}$$

$$\partial_t C_i + \bar{u}\cdot\bar{\nabla}C_i + D_i\nabla^2 C_i \tag{4}$$

where $\mu(r)$ is the spatially varying viscosity profile with r the radial coordinate in the domain and $\kappa = h^2/12$ is the permeability calculated from the Hele-Shaw cell gap h. The diffusion coefficients D_i were set as previously described and C_i are the concentration fields for H^+ and OH^-. In the convective case, the reactivity of the species was not considered as the characteristic injection times were much faster than the experimental reaction time. The estimated Damköhler number for the experiments is in the range $D_a \in (0.0005 \pm 0.0002, 0.0034 \pm 0.0015)$ (see the SI for details), thus the reaction times are much larger than the advection time.

All simulations were performed using dimensional units to facilitate direct comparison with the experiments. The inlet flow velocity at the central boundary was calculated using

$$-\bar{n}\cdot\bar{u} = v_0(Q) \tag{5}$$

where $v_0 = Q/2\pi rh$. The injection hole is the inner circular region with $r = 2$ mm.[5,26] The outlet boundary condition was set with a pressure outlet $p = 0$ Pa.

RESULTS

Experiments. Figure 2 shows the dynamics of the system when the initial concentration of formaldehyde is varied while the other reagent concentrations are kept constant ($[PAA]_0 = 0.4386$ wt %, $[SO_3^{2-}]_0 = 0.0684$ M and $[CI]_0 = 0.021$ wt %). The chemical conditions were chosen as the optimal values to maximize the differences between the initial and the final pH and viscosity in a batch reactor following ref 17. Note that the system is very sensitive to the initial chemical concentrations and, in particular, to $[PAA]_0$. Each row shows the temporal evolution of one experiment in addition to a schematic plot of the spatial viscosity profile for the same configuration. Figure 2a features the control experiment where pure water is the displaced solution. Due to the absence of reactivity between the involved solutions, the displacement is hydrodynamically stable, as the viscosity of the displacing polymeric solution is larger than that of the displaced water.

Hence, the front remains circular without any fingering instability. This behavior is coherent with the schematic viscosity profile shown in the last column of the first row, where the viscosity profile remains stable along the whole experiment due to the lack of reaction.

When the concentration of formaldehyde is nonzero in the displaced solution (Figure 2b,c), a blue contour associated to a zone of high pH can be observed in the contact zone between both liquids. This blue color witnesses the occurrence of the pH-changing reaction between formaldehyde in the displaced fluid and the sulfite dissolved in the injected solution. The thickness of this blue contour increases in time due to diffusion and reaction in the radial geometry.[26] At a fixed time, this thickness also depends on the values of the reaction parameters. Typically, in Figure 2b, although the blue contour is appreciated, the low formaldehyde concentration (0.0496 M) generates only a thin blue contour in which the viscosity increase is too low and not extended enough to trigger a viscous fingering instability (see also the schematic viscosity profile). The displacement front remains therefore essentially circular, with very small or negligible perturbations. In the last case (Figure 2c), the formaldehyde concentration is large enough (0.75 M) to generate a wider zone of larger viscosity, which makes the emergence of a well-defined fingering instability possible.

In the following sections, we will analyze the effect of varying the FS reactant concentrations and flow rate on the fingering described in Figure 2.

Initial Mixing Area Size. The dependence of the initial blue contour thickness (or initially mixed area) as a function of $[formaldehyde]_0$ and $[SO_3^{2-}]_0$ is presented in Figure 3. Panel

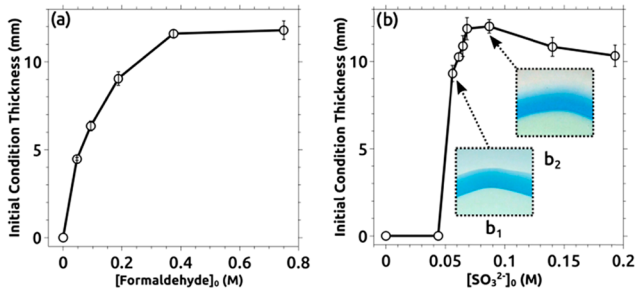

Figure 3. Initial condition thickness as a function of (a) $[formaldehyde]_0$ at $[SO_3^{2-}]_0 = 0.0684$ M and (b) $[SO_3^{2-}]_0$ at $[formaldehyde]_0 = 0.75$ M. All measurements were done 3 h after the injection in the Hele-Shaw cell of 3 mL of the displacing solution in which $[PAA]_0 = 0.4386$ wt % and $[CI]_0 = 0.021$ wt %. Insets (b_1) and (b_2) show the fuzziness at the interface for $[SO_3^{2-}]_0 = 0.0614$ M and $[SO_3^{2-}]_0 = 0.0870$ M, respectively.

(a) shows that a large increment in the thickness of the blue contour is observed when the formaldehyde initial concentration is increased. The measured thickness varies from 0 mm in the control experiment, ($[formaldehyde]_0 = 0$ M), up to an average value of 11.8 mm for $[formaldehyde]_0 = 0.75$ M. In Figure 3b, the effect on the blue contour thickness of varying sulfite concentration is shown. Low concentration values produce almost no reactivity (demonstrated in the low interface thickness) until $[SO_3^{2-}]_0 \geq 0.056$ M. Above this value, the thickness continuously increases until $[SO_3^{2-}]_0 = 0.087$ M, above which a slow decrease of the thickness is observed for the remaining values of $[SO_3^{2-}]_0$ considered. Another remarkable effect is that the blue contour becomes fuzzy for $[SO_3^{2-}]_0 \geq 0.0870$ M (inset b_2) in contrast to the sharp boundary observed for $[SO_3^{2-}]_0 = 0.0561$ M (inset b_1).

Circularity. To quantify the strength of the fingering mechanism, we measure a morphological descriptor called circularity $C = 4\pi[\text{area}/\text{perimeter}^2]$ that describes how close the boundary between the two solutions is to a perfect circle. The value of C was calculated directly using FIJI.[21] The used algorithm calculates the whole area and the perimeter of a binary mask created from the experimental and numerical patterns (details are given in the SI). Some other observables

DOI: 10.1021/acs.langmuir.8b03834
Langmuir 2019, 35, 4182−4188

were used in the literature[27,28] to describe the nature of the fingers such as density area. For our particular experiments, we found that the circularity provides a more accurate description due to the limited area where the fingers are confined (see a more detailed description in the SI).

Figure 4 shows the variation of the circularity as a function of the initial concentrations of formaldehyde and sulfate. In

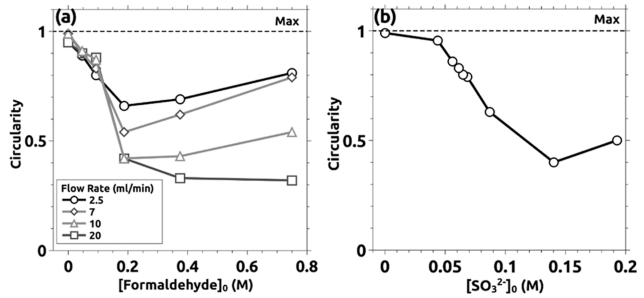

Figure 4. Circularity as a function of the initial concentration of (a) $[formaldehyde]_0$ for different flow rates and $[SO_3^{2-}]_0$ = 0.0684 M and (b) $[Sulfite]_0$ at $[formaldehyde]_0$ = 0.75 M. In all cases, $[PAA]_0$ = 0.4386 wt % and $[CI]_0$ = 0.021 wt %. The flow rate used was 7 mL/min. Values near 1 indicate that the obtained patterns are close to a perfect circle.

Figure 4a, the effect of the formaldehyde initial concentration is shown for four different flow rates at constant $[PAA]_0$ = 0.4386 wt %, $[SO_3^{2-}]_0$ = 0.0684 M, and $[CI]_0$ = 0.021 wt %. An increasing flow rate gives smaller circularity values. This result is associated with the well-known destabilizing effect of increasing the flow rate on fingering.[29]

Additionally, an increment of the formaldehyde initial concentration also destabilizes the system, allowing the generation of viscous fingering between the two solutions. For lower formaldehyde concentrations, the reaction zone is thinner, making the system more stable and, thus, the circularity value is closer to 1. Note that for all formaldehyde concentrations below 0.2 M, the larger the flow rate, the more important the destabilization is. However, for $[formaldehyde]_0$ > 0.2 M, the circularity increases again when the formaldehyde concentration is increased for all flow rates studied except for 20 mL/min. The Supporting Information contains a group of pictures showing the changes that the flow rate and the formaldehyde concentration induce in the finger shape.

Figure 4b shows the effect of changes in the sulfite initial concentration on circularity in the displacing solution, with $[PAA]_0$ and $[CI]_0$ kept constant at 0.4386 and 0.021 wt %, respectively, and $[formaldehyde]_0$ = 0.75 M. The curve exhibits barely any effect for $[SO_3^{2-}]_0$ < 0.06 M. This is coherent with the fact that batch measurements show almost no pH change in this range (see Figure 2 in ref 17). For 0.06 M < $[SO_3^{2-}]_0$ < 0.14 M, we see a decrease in circularity up to the minimum value of C = 0.4. The effect of sulfite concentration is especially complex to analyze because it does not only affect the reaction itself but also has a strong effect on the rheology[17] of the system, which, at the same time, affects the overall viscosity ratio. As previously described in ref 17, there is a particular concentration ($[SO_3^{2-}]_0$ = 0.0614 M) in a fully stirred system that maximizes the difference between the viscosity of the displacing solution and the viscosity of the blue zone. For larger concentrations, the viscosity ratio decreases due to the electrostatic quenching produced by the sodium ions over the PAA. For such cases, we expected circularity values closer to 1 for $[SO_3^{2-}]_0$ > 0.0614 M. However, we observed a continuous decrement for $[SO_3^{2-}]_0 \gg$ 0.077 M (which was the largest value analyzed in the stirred system). Additionally, we also observed the generation of the blue contour for $[SO_3^{2-}]_0$ = 0.0561 M, which also differs from the results previously reported in a homogeneous system.[17] These results are likely due to the fact that the mixing between the displacing and the displaced solution is different in the present spatially extended system where diffusion acts compared to a stirred system.

Schlieren Experiments. To enlighten the mechanisms at play in the instability, several control experiments were also performed by using a Schlieren optical technique[22] that allows direct visualization of gradients of the refractive index in the solution and, thus, to follow the flows and displacements even if they are not accompanied by color changes. Results are shown in Figure 5. Figure 5a is a snapshot of the moment

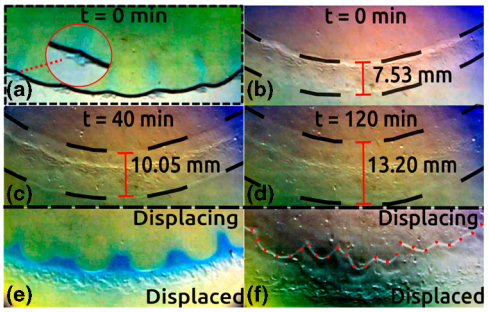

Figure 5. Experiments analyzed under the Schlieren technique. (a) Generation of the initial condition for a colored control experiment where $[PAA]_0$ = 0.4386 wt %, $[formaldehyde]_0$ = 0.1875 M, $[SO_3^{2-}]_0$ = 0.0684 M, and $[CI]_0$ = 0.021 wt %. The red circle indicates the polymer cumulus at the interface. (b–d) Temporal evolution of the initial condition in a colorless experiment, where $[PAA]_0$ = 0.4386 wt %, $[formaldehyde]_0$ = 0.1875 M, and $[SO_3^{2-}]_0$ = 0.1403 M. The red marks indicate the thickness of the reactive zone and the black dashed line indicates the limits of the reactive contour. (e) Fingering instability seen in a colored experiment. The finger propagation is blocked in the displaced solution by the polymer cumuli, which act as a barrier. (f) Fingering instability of a colorless experiment. The red dashed line indicates the finger onset. For both experiments, the flow rate was set at 7 mL/min.

where the initial condition starts to form in a control experiment with color indicator ($[formaldehyde]_0$ = 0.1875 M, $[SO_3^{2-}]_0$ = 0.0684 M, and $[CI]_0$ = 0.021 wt %). Note that small polymer accumulations appear at the interface between the displacing and displaced solutions (see the inset in red circle). The generation of these polymer aggregates, related to interface interactions between the polymer molecules in specific chemical and electrostatic conditions, can only be observed under Schlieren optics. This phenomenon is extensively described in the literature.[17,30−32] Once displaced, these cumuli generate small blue plumes across the displacing zone, indicating that its formation is produced by the reactivity between both solutions. Additionally, note that the interface becomes slightly deformed by the action of the polymer cumuli that destabilize the initially stable profile. This rippling will be essential to the development of the instability, as it produces a fluctuation in the front that helps to trigger the fingering. In Figure 5b–d, the temporal evolution of a control experiment without color indicator is presented. In this particular case, $[formaldehyde]_0$ = 0.1875 M and $[SO_3^{2-}]_0$ = 0.1403 M. Thanks to the optical technique, it is possible to appreciate

DOI: 10.1021/acs.langmuir.8b03834
Langmuir 2019, 35, 4182−4188

how the reaction contour grows in time and how its thickness enlargement is directly related to the generation of polymer aggregates (black dashed lines). Adjacent to this mark, a thickness value is presented for each case. This clearly shows how the contour becomes thicker depending on the spatial distribution of the reagents but also shows that the polymer is a fundamental factor in the overall development of instability.

Figure 5e,f compares the fingering instability when the displacing solution is injected at 7 mL/min immediately after the generation of the initial condition for a colored (Figure 5e) and a colorless (Figure 5f) experiment. Figure 5e shows how and where the fingering instability is produced. As it was described before, the generation of a reactive zone is compulsory to trigger the hydrodynamic instability. The production of the polymer accumulations continues during all the experiment, generating a more viscous and thicker layer of polymer that allows the development of fingering while blocking the fingers, flattening their tips and preventing the propagation beyond this limit. This polymer cumuli generation explains why plumes and fingers are observed for the highest concentrations of sulfite. Even if the system should be stable, the accumulation of polymer at the interface makes the finger onset possible in those experiments where the viscosity difference between the displacing and the blue contour is small. Figure 5f shows the equivalent of Figure 5e for an experiment without color indicator. The instability is delimited by a red dashed line.

Numerical Results. The kinetic model used for the reactive system is based on the clock reaction mechanism proposed by Kovacs et al.[14] The model includes neither the rheological properties of the PAA nor the secondary effects related to high sulfite concentrations.[17] Furthermore, it is intended to show only the effects associated with a classical chemo-hydrodynamic system. The polymer is, however, included implicitly in the viscosity−pH function to take into account the viscosity ratio between the displacing and the displaced solutions. Moreover, slight modifications in the reaction rate constants were included in the reaction model to match our experimental results with the simulations (see the SI for details). As it was observed in the experimental results, the blue contour is characterized by a zone with large pH, meaning that the OH^- concentration in such a location is high and increases the interface thickness along the whole experiment. Considering this and as described in the Materials and Methods section, the viscosity function was modeled as $\mu(r) = \beta 10^{\alpha[OH^-](r)}$, where r is the radial coordinate, μ is the dynamic viscosity, $\beta = 1$ Pa s is a constant related to the viscosity of the displacing solution, and $\alpha = 9 \times 10^7$ [1/M] is a constant that modulates the viscosity ratio between the displacing and blue contour zones. Both values were kept constant for all the cases studied to see the influence of $[OH^-]$ concentration on the spatial profiles.

In Figure 6, an example of a nonlinear convective simulation is presented. Figure 6a shows three time frames of the viscosity field for a simulation with initial conditions identical to those used for the experiments in Figure 2. Note that the numerical result agrees well with the experimental counterpart (Figure 2c). Two color bars are located below the time frames, indicating the pH and the viscosity ranges. The initial viscosity profile for the convective simulation is presented in Figure 6b. This profile was obtained using the reaction−diffusion model in the same way as in the experimental procedure.

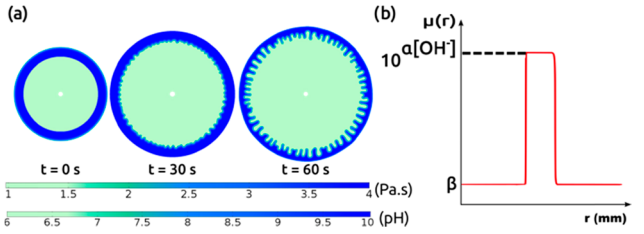

Figure 6. (a) Viscosity field for a control simulation, where $[formaldehyde]_0 = 0.75$ M, $[SO_3^{2-}]_0 = 0.0684$ M, $[HSO_3^-]_0 = 0.0533$ M, $[H^+]_0 = 1.9952 \times 10^{-7}$ M, $Q = 7$ mL/min, $D_R = 1 \times 10^{-11}$ m^2/s, and $D_D = 1 \times 10^{-9}$ m^2/s.[24] The color bars were set in accordance with the color range of the color indicator. (b) Initial viscosity profile across the radial coordinate obtained directly from the simulations. Schematics of the model definition are presented in the plot.

All the experimental results reported in Figures 3 and 4 were reproduced in silico. These results are shown in Figure 7. In

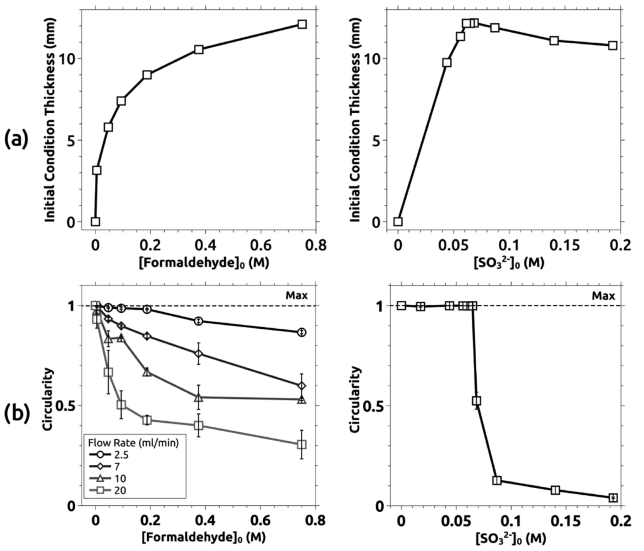

Figure 7. Simulation results: Row (a) Initial condition thickness as a function of (left column) $[formaldehyde]_0$ and (right column) $[SO_3^{2-}]_0$. All values were obtained by measuring the contour thickness generated after 3 h (simulation time). The concentration values were exactly the same in comparison with the experimental part, with the exception of $[formaldehyde]_0 = 0.005$ M. For the species inside the displaced solution, the diffusion coefficient was set as $D_D = 1 \times 10^{-9}$ m^2/s, whereas for all the species inside the displacing, the value was set as $D_R = 1 \times 10^{-11}$ m^2/s.[24] Row (b) Circularity is measured in the convective simulations as a function of (left column) $[formaldehyde]_0$ for various flow rates and (right column) $[SO_3^{2-}]_0$ for a flow rate of 7 mL/min. The maximum circularity value is indicated by the dashed line.

Figure 7a, the initial condition thickness for various formaldehyde concentrations (left column) and sulfite concentrations (right column) is presented. Figure 7b shows the effect of concentrations on circularity. Note that, in both cases, the results qualitatively agree with the experimental counterpart (see details in the SI).

DISCUSSION AND CONCLUSIONS

In the present work, we have analyzed one of the multiple applications of the coupling between a pH-sensitive polymer and a pH-changing chemical reaction. In particular, we have

DOI: 10.1021/acs.langmuir.8b03834
Langmuir 2019, 35, 4182−4188

adapted previous results obtained in a homogeneous batch system[17] into an open-flow Hele-Shaw arrangement to allow for coupling between a pH clock reactive system and a hydrodynamic instability. The aim of this work was to induce a viscous fingering instability by reaction and modulate the properties of the fingering by modifying characteristic parameters of the chemistry and the hydrodynamics. We also proposed a numerical model to confirm the experimental results and analyze the effects of chemistry. A morphological parameter was measured via image analysis to characterize the results.

A qualitative and quantitative comparison between the experiments and simulations was performed. We noticed a good agreement between results for the blue contour generation. This confirms not only that the reactive model previously reported by Kovacs et al.[14] is suitable to simulate the system previously reported by Escala et at.[17] but also that the numerical parameters were appropriate as an initial approximation. In the convective experiments, the results are in qualitative agreement, although some minor differences can be observed. In this case, it is necessary to separate the results obtained by varying $[\text{formaldehyde}]_0$ from those obtained by varying $[SO_3^{2-}]_0$. In the first case, the average circularity values obtained for high formaldehyde concentrations in the experiments and simulations are in qualitative good agreement. The numerical statistical analysis also shows that different initial conditions can vary the expected decrement in circularity. This was not observed for the sulfite case, where simulations show some differences with the experiments. In this case, the difference in the results is due to the simplicity of the proposed model that did not include the rheology of the polymer or the effect of the ionic strength, although they were analyzed in the CSTR experiments.[17] As it was previously demonstrated,[17] the electrostatic quenching produced by the increment of the ions in the displacing solutions at larger sulfite concentrations affects the rheological properties of the polymer. Even if the model shows that the $[OH^-]$ concentration increases proportionally to the sulfite concentration, the viscosity ratio between the displacing and blue zones becomes smaller. To construct a more realistic model, the α value should be varied in each simulation as a function of $[SO_3^{2-}]_0$. However, this is not an easy task to do, as the PAA has a non-Newtonian behavior and its viscosity depends on the sulfite concentration and also on the shear rate. Even if some approximation can be done by performing a rheological study of the displacing solution, it is well known that the shear rate is not constant during a radial displacement inside a Hele-Shaw cell.[5,26] Also, more information about the real concentrations at the interface between the displacing and displaced solutions must be obtained. Nevertheless, in spite of its simplicity, our model was useful in showing the main features behind the experiments. The analysis of a more complex model will be the subject of a future work.

It is noteworthy that the viscous fingering instability is here triggered by using a pH reaction only at the contact zone between the two reactant solutions. Hence, minor local changes around the miscible interface completely modify the global displacement stability, which can result in interesting applications in different contexts. In addition, the use of a pH clock reaction to influence viscous fingering paves the way for a more complex control of this hydrodynamic instability if additional reactive feedbacks could be added to trigger temporal oscillations of pH.[17]

■ ASSOCIATED CONTENT

Supporting Information

The Supporting Information is available free of charge on the ACS Publications website at DOI: 10.1021/acs.langmuir.8b03834.

Method used to calculate the circularity; elasticity effects and shear rate estimation; experimental Damköhler numbers; density area calculations; finger morphological changes due to flow rate; numerical model; reaction model; 2D convection−diffusion model; model validation; extensive comparison between simulations and experimental results; effects of reagent concentration on spatial viscosity profiles; effect of diffusion on system behavior; effect of color indicator on system's rheology (PDF)

Fingering in an experiment with a flow Q = 7 mL/min and initial concentrations as in Figure 2c (AVI)

Simulation with a flow rate Q = 7 mL/min and the same initial concentrations as in experiments (AVI)

■ AUTHOR INFORMATION

Corresponding Author

*E-mail: albertoperezmunuzuri@fas.harvard.edu.

ORCID

A. P. Muñuzuri: 0000-0002-0579-9347

Notes

The authors declare no competing financial interest.

■ ACKNOWLEDGMENTS

We gratefully acknowledge financial support by the Spanish Ministerio de Economía y Competitividad and European Regional Development Fund under contract MAT2015-71119-R AEI/FEDER, UE, and by Xunta de Galicia under Research Grant No. GPC2015/014. The authors are part of the CRETUS Strategic Partnership (AGRUP2015/02). All these programs are co-funded by FEDER (UE). A.D.W. thanks FRS-FNRS under the CONTROL PDR program for financial support. J.C.-L. thanks the Spanish Ministerio de Economía y Competitividad under contract MINECO-18-AYA2017-89121-P.

■ REFERENCES

(1) Kumar, A.; Montemagno, C.; Choi, H. Smart microparticles with a pH-responsive macropore for targeted oral drug delivery. *Sci. Rep.* **2017**, *7*, No. 3059.

(2) Liu, J.; Huang, Y.; Kumar, A.; Tan, A.; Jin, S.; Mozhi, A.; Liang, X. J. pH-sensitive nano-systems for drug delivery in cancer therapy. *Biotechnol. Adv.* **2014**, *32*, 693−710.

(3) De Wit, A. Chemo-hydrodynamic patterns in porous media. *Philos. Trans. R. Soc., A* **2016**, *374*, No. 20150419.

(4) Riolfo, L. A.; Nagatsu, Y.; Iwata, S.; Maes, R.; Trevelyan, P. M. J.; De Wit, A. Experimental evidence of reaction-driven miscible viscous fingering. *Phys. Rev. E* **2012**, *85*, No. 015304(R).

(5) Nagatsu, Y.; Matsuda, K.; Kato, Y.; Tada, Y. Experimental study on miscible viscous fingering involving viscosity changes induced by variations in chemical species concentrations due to chemical reactions. *J. Fluid Mech.* **2007**, *571*, 475−493.

(6) Nagatsu, Y.; Iguchi, C.; Matsuda, K.; Kato, Y.; Tada, Y. Miscible viscous fingering involving viscosity changes of the displacing fluid by chemical reactions. *Phys. Fluids* **2010**, *22*, No. 024101.

(7) Nagatsu, Y. Viscous fingering phenomena with chemical reactions. *Curr. Phys. Chem.* **2015**, *5*, 52−63.

DOI: 10.1021/acs.langmuir.8b03834
Langmuir 2019, 35, 4182−4188

(8) Bunton, P. H.; Tullier, M. P.; Meiburg, E.; Pojman, J. A. The effect of a crosslinking chemical reaction on pattern formation in viscous fingering of miscible fluids in a Hele-Shaw cell. *Chaos* **2017**, *27*, No. 104614.
(9) Stewart, S.; Marin, D.; Tullier, M.; Pojman, J.; Meiburg, E.; Bunton, P. Stabilization of miscible viscous fingering by a step growth polymerization reaction. *Exp. Fluids* **2018**, *59*, No. 114.
(10) De Wit, A.; Bertho, Y.; Martin, M. Viscous fingering of miscible slices. *Phys. Fluids* **2005**, *17*, No. 054114.
(11) Muggeridge, A.; Cockin, A.; Webb, K.; Frampton, H.; Collins, I.; Moulds, T.; Salino, P. Recovery rates, enhanced oil recovery and technological limits. *Philos. Trans. R. Soc., A* **2014**, *372*, No. 20120320.
(12) Hejazi, S. H.; Trevelyan, P. M.; Azaiez, J.; De Wit, A. Viscous fingering of a miscible reactive A + B → C interface: a linear stability analysis. *J. Fluid Mech.* **2010**, *652*, 501−528.
(13) Gérard, T.; De Wit, A. Miscible viscous fingering induced by a simple A + B → C chemical reaction. *Phys. Rev. E* **2009**, *79*, No. 016308.
(14) Kovacs, K.; McIlwaine, R.; Gannon, K.; Taylor, A. F.; Scott, S. K. Complex Behavior in the Formaldehyde−Sulfite Reaction. *J. Phys. Chem. A* **2005**, *109*, 283−288.
(15) Kovacs, K.; McIlwaine, R. E.; Scott, S. K.; Taylor, A. F. An organic-based pH oscillator. *J. Phys. Chem. A* **2007**, *111*, 549−551.
(16) Kovacs, K.; McIlwaine, R. E.; Scott, S. K.; Taylor, A. F. pH oscillations and bistability in the methylene glycol−sulfite−gluconolactone reaction. *Phys. Chem. Chem. Phys.* **2007**, *9*, 3711−3716.
(17) Escala, D. M.; Muñuzuri, A. P.; De Wit, A.; Carballido-Landeira, J. Temporal viscosity modulations driven by a pH sensitive polymer coupled to a pH-changing chemical reaction. *Phys. Chem. Chem. Phys.* **2017**, *19*, 11914−11919.
(18) Escala, D. M.; Budroni, M. A.; Carballido-Landeira, J.; De Wit, A.; Muñuzuri, A. P. Self-organized traveling chemo-hydrodynamic fingers triggered by a chemical oscillator. *J. Phys. Chem. Lett.* **2014**, *5*, 413−418.
(19) Budroni, M. A.; De Wit, A. Dissipative structures: From reaction-diffusion to chemo-hydrodynamic patterns. *Chaos* **2017**, *27*, No. 104617.
(20) Klotz, E.; Doyle, R.; Gross, E.; Mattson, B. The equilibrium constant for bromothymol blue: a general chemistry laboratory experiment using spectroscopy. *J. Chem. Educ.* **2011**, *88*, 637−639.
(21) Schindelin, J.; Arganda-Carreras, I.; Frise, E.; et al. Fiji: an open-source platform for biological-image analysis. *Nat. Methods* **2012**, *9*, 676−682.
(22) Bunton, P.; Marin, D.; Stewart, S.; Meiburg, E.; De Wit, A. Schlieren imaging of viscous fingering in a horizontal Hele-Shaw cell. *Exp. Fluids* **2016**, *57*, No. 28.
(23) Settles, G. S. *Schlieren and Shadowgraph Techniques: Visualizing Phenomena in Transparent Media*; Springer Science & Business Media, 2012.
(24) Adamczyk, Z.; Bratek, A.; Jachimska, B.; Jasiński, T.; Warszyński, P. Structure of poly(acrylic acid) in electrolyte solutions determined from simulations and viscosity measurements. *J. Phys. Chem. B* **2006**, *110*, 22426−22435.
(25) Li, J.; Rivière, B. Numerical modeling of miscible viscous fingering instabilities by high-order methods. *Transp. Porous Media* **2016**, *113*, 607−628.
(26) Brau, F.; Schuszter, G.; De Wit, A. Flow control of A + B → C fronts by radial injection. *Phys. Rev. Lett.* **2017**, *118*, No. 134101.
(27) Nagatsu, Y.; Kondo, Y.; Kato, Y.; Tada, Y. Effects of moderate Damköhler number on miscible viscous fingering involving viscosity decrease due to a chemical reaction. *J. Fluid Mech.* **2009**, *625*, 97−124.
(28) Fernandez, J.; Homsy, G. Viscous fingering with chemical reaction: Effect of in-situ production of surfactants. *J. Fluid Mech.* **2003**, *480*, 267−281.
(29) Homsy, G. M. Viscous fingering in porous media. *Annu. Rev. Fluid Mech.* **1987**, *19*, 271−311.
(30) Teraoka, A. A.; Teraoka, I. *Polymer Solutions: An Introduction to Physical Properties*; John Wiley & Sons, 2002.
(31) Palencia, M.; Rivas, B. L. Adsorption of linear polymers on polyethersulfone membranes: Contribution of divalent counterions on modifying of hydrophilic−lipophilic balance of polyelectrolyte chain. *J. Membr. Sci.* **2011**, *372*, 355−365.
(32) Kobayashi, S.; Müllen, K. *Encyclopedia of Polymeric Nanomaterials*; Springer, 2015; pp 1654−1658.

DOI: 10.1021/acs.langmuir.8b03834
Langmuir 2019, 35, 4182−4188